Solid State Communications 149 (2009) 2181–2184

Contents lists available at ScienceDirect

Solid State Communications

journal homepage: www.elsevier.com/locate/ssc

On the low-temperature properties of $TmRu_2Si_2$

Łukasz Gondek [a,*], Dariusz Kaczorowski [b], Andrzej Szytuła [c]

[a] Faculty of Physics and Applied Computer Science, AGH University of Science and Technology, Mickiewicza 30, 30-059 Kraków, Poland
[b] Institute of Low Temperature and Structure Research, Polish Academy of Sciences, P.O.Box 1410, 50-950 Wrocław, Poland
[c] M. Smoluchowski Institute of Physics, Jagiellonian University, Reymonta 4, 30-059 Kraków, Poland

ARTICLE INFO

Article history:
Received 3 June 2009
Received in revised form
9 September 2009
Accepted 14 September 2009 by C. Lacroix
Available online 18 September 2009

PACS:
72.15.-v
75.20.Hr
75.30.Cr
75.40.Cx

Keywords:
A. Metals
D. Electronic transport
D. Heat capacity
D. Thermodynamic properties

ABSTRACT

Magnetic, electrical transport and heat capacity measurements have been performed on polycrystalline sample of the compound $TmRu_2Si_2$, which crystallizes with the tetragonal $ThCr_2Si_2$-type crystal structure. The results show paramagnetic behaviour down to 0.3 K, at variance with the literature data. On the basis of the collected data, possible origins of non-magnetic behaviour are discussed. Mixed valence of Tm ions or hybridisation between Tm 4f and Ru 4d states are the most probable reasons for paramagnetic behaviour of the $TmRu_2Si_2$.

© 2009 Elsevier Ltd. All rights reserved.

1. Introduction

The RRu_2Si_2 (R — rare earth) compounds form with a tetragonal body-centred crystal structure (space group I4/mmm) of the $ThCr_2Si_2$-type. They exhibit a large variety of intriguing magnetic properties [1,2]. $CeRu_2Si_2$ is a heavy fermion system with strongly enhanced electronic specific heat coefficient of 389 mJ/(mol K^2) at low temperatures [3]. For $PrRu_2Si_2$ complex magnetic behaviour was reported, with ferromagnetic ordering below 14 K and antiferromagnetic order characterised by incommensurate sine-wave magnetic structure in a narrow temperature range 14–16 K [4]. Similar magnetic properties were observed for $NdRu_2Si_2$: below 9 K the compound exhibits ferromagnetism, whereas above this temperature up to 24 K an antiferromagnetic arrangement of the Nd magnetic moments occurs [5]. In turn, $SmRu_2Si_2$ and $EuRu_2Si_2$ are antiferromagnets with the Néel temperatures of 7 K [1] and 78 K [2], respectively. $GdRu_2Si_2$ exhibits antiferromagnetic ordering below 31 K, with strongly anisotropic magnetic behaviour [6,7]. $TbRu_2Si_2$ and $DyRu_2Si_2$ order antiferromagnetically at $T_N = 57$ K and 29 K, respectively [5,8,9]. In $TbRu_2Si_2$, upon decreasing temperature the sine-modulated structure turns into a squared one [8]. Also $HoRu_2Si_2$ and $ErRu_2Si_2$ order antiferromagnetically. Their critical temperatures are 18.6 K [10] and 6 K [11], respectively.

Some limited magnetic data for $TmRu_2Si_2$ were published in Ref. [1]. The authors communicated that this silicide orders ferromagnetically at about 1 K. However, their measurements were performed down to 1.5 K only. The ordering temperatures in other TmT_2Si_2 silicides with different d-electron transition metals (T) are also small (3 K for T = Co, 2.7 K for T = Ni, 3.6 K for T = Cu, about 4.2 K for T = Rh, and 1 K for T = Os) [12]. Apparently, the magnetic interactions between the Tm magnetic moments are relatively weak in all these phases. A possible reason for the observed behaviour is the presence of a singlet ground state. In such a case, long-range magnetic order has an induced nature, with excited crystal field (CF) levels being involved in the appearance of magnetic ordering.

In this paper we revisit the low-temperature physical properties of $TmRu_2Si_2$ by means of magnetic susceptibility, electrical resistivity and specific heat measurements. Our studies have been performed at temperatures down to 0.3 K, with the main aim of attesting the occurrence of the magnetic phase transition at 1 K, reported in Ref. [1].

2. Experimental details

Polycrystalline sample of $TmRu_2Si_2$ was prepared by arc melting the elemental constituents of high purity (Tm:99.9 wt%;

* Corresponding author.
E-mail address: lgondek@agh.edu.pl (Ł. Gondek).

0038-1098/$ – see front matter © 2009 Elsevier Ltd. All rights reserved.
doi:10.1016/j.ssc.2009.09.017

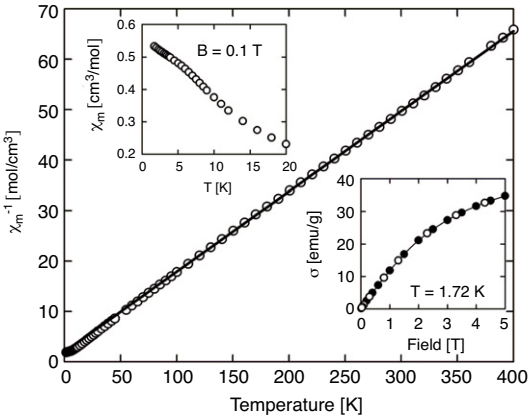

Fig. 1. Temperature dependence of the magnetic susceptibility of $TmRu_2Si_2$. The solid line marks the Curie–Weiss behaviour discussed in the text. The upper inset shows the low-temperature susceptibility. The lower inset displays the isothermal magnetisation measured at 1.72 K with increasing (open symbols) and decreasing (filled symbols) magnetic field.

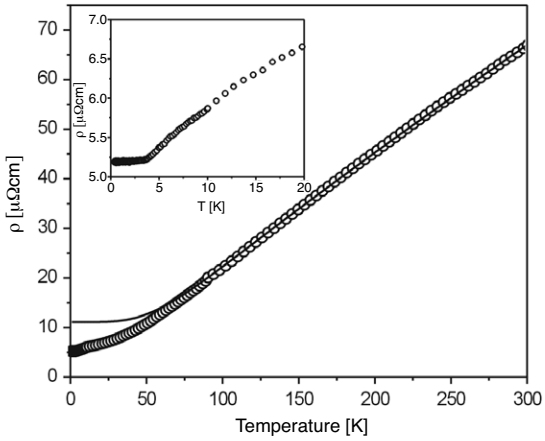

Fig. 2. Temperature dependence of the electrical resistivity of $TmRu_2Si_2$. The solid line represents the fit of the Bloch–Grüneisen model to the experimental data. The inset shows the low-temperature behaviour of the resistivity on a semilogarithmic scale.

Ru:99.99 wt%; Si:99.99 wt%) under titanium-gettered argon atmosphere. The ingot was re-melted several times in order to ensure good homogeneity. Then the product was annealed in an evacuated silica tube at 870 K for 100 h.

The quality of the obtained sample was checked by X-ray powder diffraction at room temperature using a Philips PW-3710 X'PERT diffractometer with Cu Kα radiation. It was confirmed that $TmRu_2Si_2$ crystallises with the $ThCr_2Si_2$-type tetragonal structure with the lattice parameters $a = 4.138(4)$ Å and $c = 9.469(9)$ Å, in agreement with the data reported in Ref. [1]. Two peaks of very low intensities, that could not be indexed, appeared at a 2θ angle of 30.75° and 34.14°. The amount of this impurity was estimated to be less than 1%. It was not possible to identify that spurious phase. However, the appearance of the constituting elements and their oxides were excluded.

Magnetic measurements were carried out in the temperature range 1.7–400 K in magnetic fields up to 5 T using a Quantum Design MPMS-5 SQUID magnetometer. Electrical resistivity and heat capacity studies were made over the interval 0.35–300 K employing a Quantum Design PPMS platform. The electrical resistivity was measured using a standard four-point ac technique. The electrical leads were attached to the specimen by spot welding. The specific heat was taken by relaxation method.

3. Results

3.1. Magnetic properties

The magnetic data of $TmRu_2Si_2$ are summarised in Fig. 1. Above about 50 K, the inverse magnetic susceptibility obeys the Curie–Weiss law with the effective magnetic moment $\mu_{eff} = 7.1$ (1) μ_B and the paramagnetic Curie temperature $\theta_p = -12.5(2)$ K. At lower temperatures some small departure from the straight-line behaviour is observed, which can be attributed to crystal field effects. The derived magnitude of μ_{eff} is somewhat lower than that expected for Tm^{3+} free ion (7.56 μ_B). Slightly higher value of 7.38 μ_B was reported in Ref. [1]. On the other hand, the value of θ_p given in the latter paper is as large as +65.7 K, being rather inconsistent with the claimed ferromagnetic order at about 1 K. The problem may be caused by the fact that θ_p was extrapolated in Ref. [1] from very high temperatures (300–1100 K).

As shown in the upper inset to Fig. 1, down to 1.7 K no clear evidence of any magnetic transition is visible. The magnetic susceptibility exhibits a tiny hump below 10 K that likely manifests CF interactions, evidenced in the heat capacity data (see Section 3.3). The other inset in Fig. 1 presents the isothermal magnetisation curve measured at 1.72 K. It bends in strong magnetic fields, in a manner typical of paramagnetic state. In a magnetic field of 5 T, the magnetic moment is equal to 2.7 μ_B.

3.2. Electrical resistivity

The temperature variation of the electrical resistivity of $TmRu_2Si_2$ is displayed in Fig. 2. Clearly, no sign of any magnetic ordering is visible on the $\rho(T)$ curve down to the lowest reached temperature of 0.35 K (see the inset to Fig. 2). The shape of the curve below roughly 100 K is governed by the CF effects. Namely, the spin-disorder resistivity is strongly temperature dependent. Above about 100 K, the resistivity increases with rising temperature in a quasi-linear manner. In this temperature range, it can be assumed that the CF effects in the compound studied (cf. Section 3.3) have only a minor influence on $\rho(T)$, i.e. the spin-disorder resistivity is roughly constant. In such a case, the resistivity can be described by the Bloch–Grüneisen (BG) formula:

$$\rho(T) = (\rho_0 + \rho_\infty) + 4RT\left(\frac{T}{\Theta_D}\right)^4 \int_0^{\frac{\Theta_D}{T}} \frac{x^5 dx}{(e^x - 1)(1 - e^{-x})}, \quad (1)$$

where the first term is the sum of contribution due to the scattering conduction electrons on static defects in the crystal lattice (the residual resistivity ρ_0) and on disordered magnetic moments (the spin-disorder resistivity ρ_∞), whereas the second one represents the electron–phonon scattering (Θ_D is the Debye temperature). Fitting the BG formula to the experimental data above 100 K yielded the following set of parameters: $\rho_0 + \rho_\infty = 11(1)$ $\mu\Omega$cm, $R = 0.21(1)$ $\mu\Omega$ cm/K, $\Theta_D = 342(1)$ K. With $\rho_0 = 5.2$ $\mu\Omega$ cm, as given by the saturation of the resistivity at the lowest temperatures (see the inset), one obtains an estimate for the magnetic contribution at high temperatures $\rho_\infty = 5.9$ $\mu\Omega$ cm.

3.3. Heat capacity

The specific heat of $TmRu_2Si_2$ is presented in Fig. 3. At room temperature, it is slightly smaller than the limit given by the Dulong–Petit law. With decreasing temperature the specific heat changes in a regular way, characteristic of dominant phonon contribution. However, below 12 K some anomalous behaviour is seen, namely $C(T)$ forms a broad maximum. As discussed in the following part of the paragraph, this feature manifests the CF interactions thatgive rise to a Schottky contribution to the

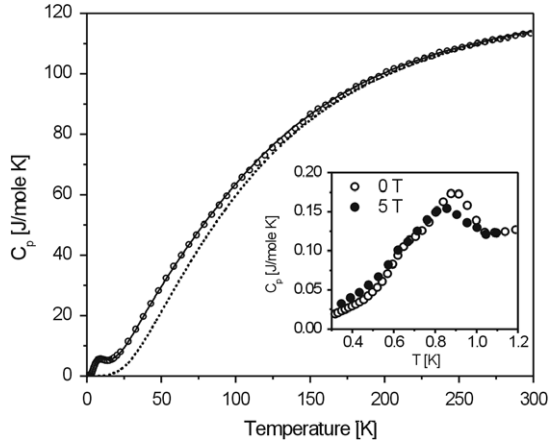

Fig. 3. Temperature dependence of the specific heat of $TmRu_2Si_2$. The solid line represents the fit of Eq. (2) to the experimental data, discussed in the text. The dotted line marks the non-magnetic contribution. The inset displays the specific heat data at the lowest temperatures, measured in zero magnetic field (open symbols) and in applied field of 5 T (filled symbols).

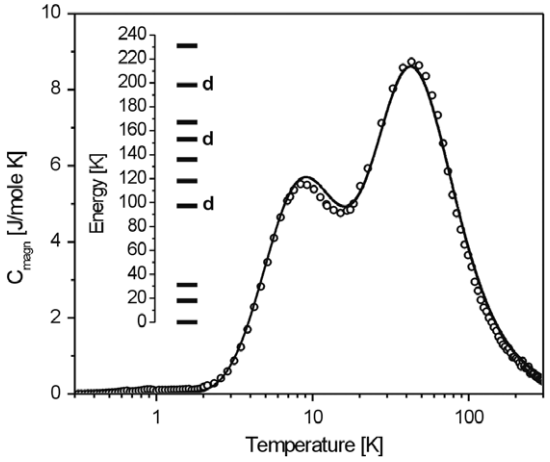

Fig. 4. Temperature dependence of the magnetic contribution to the specific heat of $TmRu_2Si_2$, derived as discussed in the text. The solid line represents the estimated Schottky contribution (see the text for details). The inset shows the corresponding crystal field splitting scheme (doublets are denoted by "d").

specific heat. At lower temperatures, further very weak anomalies are observed in the $C(T)$ curve (i.e. below 1 K it exhibits a tiny maximum, and at 0.6 K a little kink is seen (cf. the inset to Fig. 3)). The entropy associated with those transitions is 0.0084 J/mol K only. The extremely small magnitude of both singularities suggests that none of them is intrinsic to the compound studied. For example, in the isostructural silicide $TmCu_2Si_2$ the specific heat peak at the magnetic phase transition [13] is over 20 times higher than that found in our sample of $TmRu_2Si_2$. Likely, the observed features are due to the impurities evidenced on the X-ray diffraction pattern (see Section 2). Though they could not be identified, the response of their specific heat to applied magnetic field (see the inset to Fig. 3) hints at their antiferromagnetic character.

Neglecting the minor features below 1 K, the specific heat of $TmRu_2Si_2$ can by analysed by formula:

$$C_{ph+el} = 9R\left(\frac{T}{\Theta_D}\right)^3 \int_0^{\frac{\Theta_D}{T}} \frac{x^4 e^x}{(e^x-1)^2} dx + R\sum_i \frac{(\frac{\Theta_{Ei}}{T})^2 e^{\frac{\Theta_{Ei}}{T}}}{(e^{\frac{\Theta_{Ei}}{T}}-1)^2} + \gamma T + \frac{R}{T^2}\left[\frac{\sum_{i=1}^{13}\delta_i^2 e^{-\frac{\delta_i}{T}}}{\sum_{i=1}^{13} e^{-\frac{\delta_i}{T}}} - \left(\frac{\sum_{i=1}^{13}\delta_i e^{-\frac{\delta_i}{T}}}{\sum_{i=1}^{13} e^{-\frac{\delta_i}{T}}}\right)^2\right] \quad (2)$$

where Θ_D is the Debye temperature, Θ_{Ei} are the Einstein temperatures, γ is the electronic specific heat coefficient, R is the gas constant and δ_i are the energies of crystal field levels (in kelvin). For the investigated compound there are 3 acoustic modes (described by the first term of Eq. (2)) and 12 optical modes (described by the second term of Eq. (2)). For simplicity of the refinement, the optical modes were grouped into four triple-degenerated branches. The third term of Eq. (2) represents the electronic specific heat, while the last term accounts for the Schottky contribution. Fitting the above formula to the experimental data yielded the phonon contribution, as displayed in Fig. 3 by the dotted line, and the magnetic contribution as presented in Fig. 4. The so-obtained values of the Debye and Einstein temperatures are gathered in Table 1. The average over Θ_D and Θ_E's amounts to 348 K, i.e. it is very close to the characteristic temperature of the lattice vibrations derived from the electrical resistivity data. The electronic contribution to the specific heat of $TmRu_2Si_2$ is quantified by $\gamma = 9.1(1)$ mJ/mol K^2, which is a typical value for rare-earth intermetallics without magnetic ordering.

Table 1
Results of the specific heat analysis of $TmRu_2Si_2$. Characteristic temperatures Θ_D and Θ_{E1} describe phonons within Debye and Einstein regimes, respectively. γ is the Sommerfeld coefficient of the electronic specific heat.

Θ_D (K)	265.1(3)
Θ_{E1} (K)	173.9(2)
Θ_{E2} (K)	299.1(8)
Θ_{E3} (K)	448(2)
Θ_{E4} (K)	552(3)
γ (mJ/mol K^2)	9.1(1)

As is apparent from Fig. 4, the obtained magnetic specific heat can be well modelled by the CF scheme presented in the inset. In the tetragonal crystal field potential, the ground multiplet $^3H_6$ of Tm^{3+} ions splits into 7 singlets and 3 doublets. The overall CF splitting was found to be about 230 K. The ground energy level is a singlet, however the first excited state (another singlet) is located only less than 20 K above the ground state. The derived CF model nicely describes the $C_{magn}(T)$ curve of $TmRu_2Si_2$, in particular the specific heat maximum observed below 10 K. Moreover, it is consistent with the data available for other TmT_2Si_2 silicides. In those phases the overall CF splitting was found to be 275 K for T = Fe [14], 292 K for T = Co [15], 154 for T = Ni [15] and 181 K for T = Cu [16].

Fig. 5 presents the magnetic entropy in $TmRu_2Si_2$, calculated as $S_{magn}(T) = \int_0^T (C_{magn}(T')/T')dT'$. At room temperature S_{magn} saturates at a value close to Rln13, expected as the high-temperature limit for the $^3H_6$ multiplet.

4. Concluding remarks

The low-temperature data obtained for $TmRu_2Si_2$ have not confirmed the occurrence of ferromagnetic state below 1 K, which was postulated in Ref. [1]. The electrical resistivity of the measured sample is featureless around 1 K and does not exhibit any hint at magnetic ordering down to the lowest reached temperature of 0.35 K. Though the specific heat does show a small anomaly at 1 K, this feature has an antiferromagnetic character, and its magnitude is too small to be an intrinsic property of $TmRu_2Si_2$.

The lack of magnetic ordering in the compound studied is rather surprising. It is unlikely that the ordered state is avoided because of the presence of a singlet as the crystal field ground state, because the first excited CF level lies close enough in energy (less than

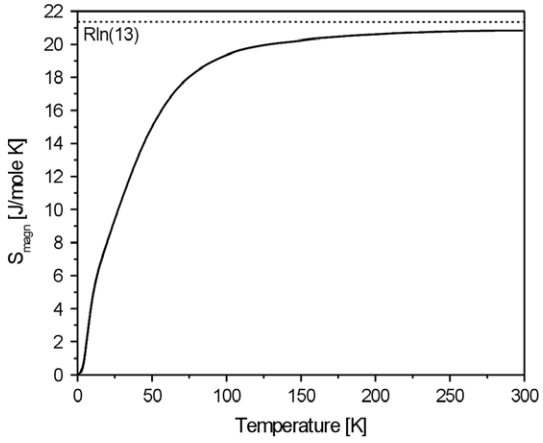

Fig. 5. Temperature variation of the magnetic entropy of $TmRu_2Si_2$, calculated from the specific heat data shown in Fig. 4.

20 K) to establish magnetic order. Also the Kondo interactions can be ruled out as a possible reason for suppressed magnetism in $TmRu_2Si_2$, which exhibits a simple metallic character of the electrical conductivity and quite small electronic contribution to the specific heat. Actually, heavy-fermion behaviour is extremely rare within Tm-based compounds [17].

In view of the above, it seems possible that the paramagnetic character of $TmRu_2Si_2$ has its origin in the tendency of Tm ions to show mixed-valence states. The valence fluctuations between $4f^{12}$ and $4f^{13}$ configurations, related to Tm^{3+} and Tm^{4+} ions, respectively, are known to bring about unusual magnetic behaviour [18]. As both configurations possess non-zero total angular momentum ($J = 6$ for Tm^{3+} and $J = 7/2$ for Tm^{2+}), in mixed valent Tm-based compounds, the effective magnetic moment is only slightly reduced in comparison to that expected within the Russell–Sounders coupling for trivalent Tm ion. In the case of $TmRu_2Si_2$ the experimentally determined value of the effective magnetic moment would correspond to the mean valance +2.85. Another possible rationale for the absence of magnetic order in the investigated compound is the role played by hybridisation of the Tm 4f electronic states with the Ru 4d orbitals. Recently, a similar effect was shown to be a likely origin for the non-magnetic properties of some Pr-based intermetallics [19].

Acknowledgments

This work was partially supported by the National Scientific Network "Strongly correlated materials: preparation, fundamental research and applications".

References

[1] K. Hiebl, C. Horvath, P. Rogl, M. Sienko, J. Magn. Magn. Mater. 37 (1983) 287.
[2] I. Felner, I. Nowik, J. Phys. Chem. Solids 45 (1984) 419.
[3] J.D. Thompson, J.O. Willis, C. Godart, D.E. Mac-Laughlin, L.C. Gupta, Solid State Commun. 56 (1985) 169.
[4] A.M. Mulders, A. Yaouanc, P. Dalmas de Réotier, P.C.M. Gubbens, A.A Molenaar, B. Fåk, E. Ressouche, K. Prokeš, A.A. Menovsky, K.H.J. Buschow, Phys. Rev. B 56 (1997) 8752.
[5] B. Chevalier, J. Etourneau, P. Hagenmuller, S. Quezel, J. Rossat-Mignod, J. Less-Common Met. 111 (1985) 161.
[6] G. Czjzek, V. Oestereich, H. Schmidt, K. Łątka, K. Tomala, J. Magn. Magn. Mater. 79 (1989) 42.
[7] A. Garnier, N. Gignoux, N. Iwata, D. Schmitt, T. Shigeoka, F.Y. Zhang, J. Magn. Magn. Mater. 140–144 (1995) 897.
[8] M. Ślaski, J. Leciejewicz, A. Szytuła, J. Magn. Magn. Mater. 39 (1983) 268.
[9] B. Andreani, G.F.L. Fragla, A. Garnier, D. Gignoux, D. Maurin, D. Schmitt, T. Shigeoka, J. Phys.: Condens. Matter 7 (1995) 1889.
[10] T. Shigeoka, D. Gignoux, D. Schmitt, J. Magn. Magn. Mater. 226–230 (2001) 1165.
[11] A. Blaise, R. Kmieć, B. Malaman, F. Ressouche, J.P. Sanchez, K. Tomala, G. Venturini, J. Magn. Magn. Mater. 135 (1994) 171.
[12] A. Szytuła, J. Leciejewicz, Handbook of Crystal Structures and Magnetic Properties of Rare Earth Intermetallics, CRC Press, Boca Raton, 1994.
[13] G.A. Stewart, J. Żukrowski, A. Kozłowski, Hyperfine Interact. 40 (1988) 433.
[14] D.R. Noakes, A.M. Umarji, G.K. Shenoy, J. Magn. Magn. Mater. 39 (1983) 309.
[15] S.J. Harker, B.D. van Dijk, A.M. Mulders, P.C.M. Gubbens, G.A. Stewart, C.F. de Vroege, K.H.J. Buschow, J. Phys.: Condens. Matter 14 (2002) 2705.
[16] M. Kosaka, H. Onodera, K. Ohoyama, M. Ohashi, Y. Yamaguchi, S. Nakamura, T. Goto, J. Phys. Soc. Japan 66 (1997) 2844.
[17] K. Tatematsu, N. Takeda, Y. Araki, K. Fukuda, Y. Yamada, T. Nishioka, K. Kodama, K. Shimzu, T. Matsushita, N. Wada, S. Narazu, T. Takabatake, J. Phys. Soc. Japan 77 (Suppl. A) (2008) 353.
[18] T. Saso, J. Phys. Soc. Japan 58 (1989) 4064.
[19] Ł. Gondek, A. Szytuła, D. Kaczorowski, K. Nenkov, Solid State Commun. 142 (2007) 556.